FFT SIMULATIONS AND MULTI-COATED INCLUSION MODEL FOR MACROSCOPIC CONDUCTIVITY OF 2D SUSPENSIONS OF COMPOUND INCLUSIONS

Nguyen Van Luat[1]**, Nguyen Trung Kien**[2,*]
[1]*Hanoi University of Industry, Vietnam*
[2]*University of Transport and Communication, Hanoi, Vietnam*
*E-mail: ntkien@utc.edu.vn
Received October 22, 2014

Abstract. Article introduces the Fast-Fourier transformation method (FFT) and an approximation method to calculate the conductivity of compound-inclusion composites in two-dimensional space. The approximation compares favorably with the numerical results for a number of periodic and random models over a range of volume proportions of phases, but divers at large volume proportions of the included phases when the interactions between the inclusions are more pronounced.

Keywords: Effective conductivity, Fast Fourier methods, matrix composite, coated-inclusion.

1. INTRODUCTION

Theoretical determination the effective conductivity of heterogeneous materials is usually complicated due to the complexity of the microstructure and limited information about the composites, such as the properties and volume proportions of the component materials. An approach to the problem is to construct upper and lower bounds based on the variational formulations [1, 2]. Matrix-particulate composite are suspensions of particle-inclusions in a continuous materials. In many cases the inclusions have the structure that can be presented as multi-coated inclusions. A simplest 2D model for such composites are multi-coated circle assemblage model, when the matrix phase is described as the outermost circular cell - an extension of Hashin-Shtrikman two-phase circle assemblage. More accurate estimations in particular cases would require more detailed numerical simulations. In this work we apply both numerical FFT method and the simple multi-coated circle assemblage approximation to investigate some periodic and random microstructures.

2. FAST FOURIER METHOD IN HOMOGENIZATION

The main principles of the Fast Fourier method have been presented in previous studies [3,4] (see more [5,6], in this section, we briefly recall the algorithm for composites with coated.
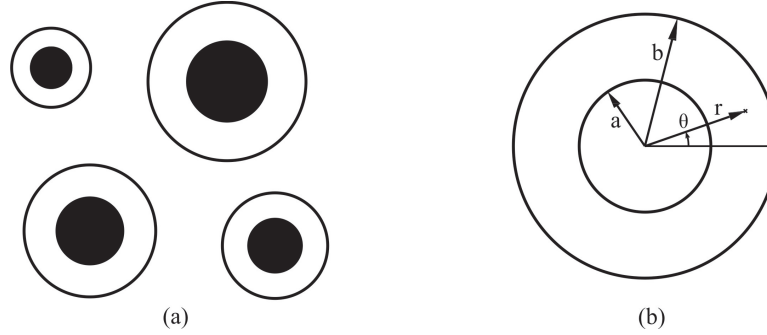
Fig. 1. (a) Three components suspension of coated inclusion; (b) A coated inclusion

Due to the periodicity of the microstructures, one can consider an unit cell as a representative volume element (RVE), which consists of a matrix medium (M) and coated inclusion component ($I = I_1 \cup I_2$) (see Fig. 1). Behavior of the component materials is described by Fourier's law

$$\mathbf{J}(\mathbf{x}) = -C(\mathbf{x}).\mathbf{E}(\mathbf{x}), \tag{1}$$

where $\mathbf{E}(\mathbf{x})$ and $\mathbf{J}(\mathbf{x})$ are respectively the local temperature gradient and thermal flux; $C(\mathbf{x})$ is the second order local conductivity tensor

$$C(\mathbf{x}) = \sum_{\alpha=1}^{n} C_\alpha I_\alpha(\mathbf{x}), \tag{2}$$

$$\mathcal{I}_\alpha(\mathbf{x}) = \begin{cases} 1 & \text{if} \quad \mathbf{x} \in V_\alpha \\ 0 & \text{if} \quad \mathbf{x} \notin V_\alpha \end{cases} \tag{3}$$

α designates the phase ($\alpha = I_1; I_2$ or M).

Following [4], the problem in a unit cell is solved by explicit recurrence process

$$\begin{cases} \mathbf{E}^{i+1}(\mathbf{x}) = \mathbf{E}^i(\mathbf{x}) - \Gamma^0(\mathbf{x}) * [C(\mathbf{x}).\mathbf{E}(\mathbf{x})] & \text{in the real space} \\ \mathbf{E}^{i+1}(\xi) = \mathbf{E}^i(\xi) - \Gamma^0(\xi).\mathbf{J}^i(\xi) & \text{in the Fourier space} \end{cases} \tag{4}$$

in which $\Gamma^0(\xi)$ is the Green operator, given by

$$\Gamma^0(\xi) = \frac{\xi \otimes \xi}{\xi \cdot C^0 \xi} \tag{5}$$

C^0 is the conductivity of the reference medium; $\mathbf{J}^i(\xi)$ and $\mathbf{E}^i(\xi)$ are respectively Fourier transformation of $\mathbf{J}^i(\mathbf{x})$ and $\mathbf{E}^i(\mathbf{x})$. Relationship between $\mathbf{J}^i(\xi)$ and $\mathbf{E}^i(\xi)$ is described by expression

$$\mathbf{J}^i(\xi) = C(\xi) * \mathbf{E}^i(\xi), \tag{6}$$

where the symbol "*" designates the product of convolution. The Fourier transformation of conductivity tensor is

$$C(\xi) = \int_V C(\mathbf{x})e^{i\xi x}dV = \sum_\alpha C_\alpha \mathcal{I}_\alpha(\xi), \tag{7}$$

$\mathcal{I}_\alpha(\xi)$ defined by

$$\mathcal{I}_\alpha(\xi) = \frac{1}{V}\int_{V_\alpha} e^{i\xi x}dV. \tag{8}$$

In the case of coated inclusion, one has the exact expression of $\mathcal{I}_\alpha(\xi)$

$$\mathcal{I}_{I2}(\xi) = \frac{\pi a}{2S\|\xi\|}J_1(a\|\xi\|)\sum_k e^{i\xi \mathbf{X}_k}, \tag{9}$$

$$\mathcal{I}_{I1}(\xi) = \frac{\pi}{2S\|\xi\|}\Big[bJ_1(b\|\xi\|) - aJ_1(a\|\xi\|)\Big]\sum_k e^{i\xi \mathbf{X}_k}, \tag{10}$$

where S is the area of unit-cell; a, b are the inner and outer radii of coated-inclusion; $\mathbf{X}_k$ is the center of coated-inclusion; J_1 is the Bessel function of first kind and first order. $\mathcal{I}_M(\xi)$ can be derived from relation

$$\sum_\alpha \mathcal{I}_\alpha(\xi) = 0, \quad \forall \xi \neq 0. \tag{11}$$

For $\xi = 0$, one have $\mathcal{I}_\alpha(0) = V_\alpha$. After replacing Eqs. (6), (7) in (4), one obtains

$$\mathbf{E}^{i+1}(\xi) = \mathbf{E}^i(\xi) - \mathbf{\Gamma}^0(\xi).\sum_\alpha C_\alpha(\mathcal{I}_\alpha * \mathbf{E}^i)(\xi). \tag{12}$$

For the three-component medium considered, the expression (12) can be written as

$$\mathbf{E}^{i+1}(\xi) = \mathbf{E}^i(\xi) - \mathbf{\Gamma}^0(\xi).\Big[C_M\mathbf{E}^i + (C_{I1} - C_M)(\mathcal{I}_{I1} * \mathbf{E}^i) + (C_{I2} - C_M)(\mathcal{I}_{I2} * \mathbf{E}^i)\Big]. \tag{13}$$

Let the unit-cell be subjected to the macroscopic temperature gradient $\mathbf{E}^0$. At convergence of the iterative process, one finds

$$\mathbf{Q} = \mathbf{J}(\xi = 0) = C^{eff}\mathbf{E}^0, \tag{14}$$

in which C^{eff} is the effective conductivity tensor. The numerical algorithm is given as follows

$$\text{Iteration } i = 1: \quad \mathbf{E}^1(\xi) = 0 \quad \forall \xi \neq 0; \quad \mathbf{E}^1(0) = \mathbf{E}^0$$
$$\mathbf{J}^1(\xi) = C(\xi) * \mathbf{E}^1(\xi)$$
$$\text{Iteration } i: \quad \mathbf{E}^i(\xi) \text{ and } \mathbf{J}^i(\xi) \text{ are known convergence test}$$
$$\mathbf{E}^{i+1}(\xi) = \mathbf{E}^i(\xi) - \mathbf{\Gamma}^0(\xi).\mathbf{J}^i(\xi)$$
$$\mathbf{J}^{i+1}(\xi) = C(\xi) * \mathbf{E}^{i+1}(\xi)$$

The convergence of the iterative procedure is reached when

$$\frac{\|\mathbf{J}^{i+1}(\xi) - \mathbf{J}^i(\xi)\|}{\|\mathbf{J}^i(\xi)\|} < \epsilon, \tag{15}$$

where ϵ is a prescribed value (10^{-3} in the present work).

3. MULTI-COATED INCLUSION MODEL

Consider a multi-coated circle model, where the disks made of material-1 (I_1) are embedded in the circular shells of material-2 (I_2), the latter are embedded in the circular shell of material-3 (M), and all composite circles of all possible sizes but with the same
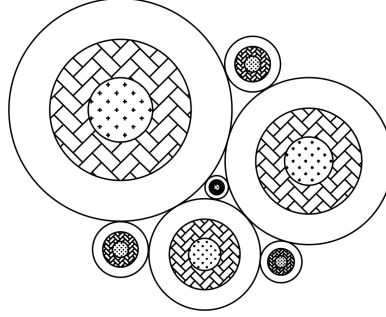
Fig. 2. Doubly-coated circles

volume proportions of phases fill all the material space (Fig. 2), and the relative volume proportions and coating orders of the phases in all n-compound spheres are the same. Macroscopic conductivity tensor of the model can be estimated by three-point correlation bounds for general isotropic multi-component materials [7]

$$(C_R^{-1} - \bar{\mathbf{v}}_c' \cdot \overline{\boldsymbol{\mathcal{A}}}_c^{-1} \cdot \bar{\mathbf{v}}_c)^{-1} \leq C^{eff} \leq C_v - \mathbf{v}_c' \cdot \boldsymbol{\mathcal{A}}_c^{-1} \cdot \mathbf{v}_c \,, \tag{16}$$

where C_V and C_R are respectively Voigt and Reuss average and

$$\mathbf{v}_c = \left\{ \frac{1}{2} v_1 (C_1 - C_R), \ldots, \frac{1}{2} v_n (C_n - C_R) \right\}^T , \tag{17}$$

$$\mathbf{v}_c' = \left\{ \frac{1}{2} v_1 C_1, \ldots, \frac{1}{2} v_n C_n \right\}^T , \tag{18}$$

$$\boldsymbol{\mathcal{A}}_c = \{ \boldsymbol{\mathcal{A}}_{\alpha\beta}^c \} , \quad \alpha, \beta = 1, \ldots, n$$

$$\boldsymbol{\mathcal{A}}_{\alpha\beta}^c = \frac{1}{4} v_\alpha C_\alpha \delta_{\alpha\beta} + \frac{1}{2} \sum_{\gamma=1}^{n} \left(A_\gamma^{\alpha\beta} - v_\alpha C_R \sum_{\delta=1}^{n} C_\delta^{-1} A_\gamma^{\delta\beta} \right) C_\gamma , \tag{19}$$

$$\bar{\mathbf{v}}_c = \left\{ \frac{1}{2} v_1 (C_V^{-1} - C_1^{-1}), \ldots, \frac{1}{2} v_n (C_V^{-1} - C_n^{-1}) \right\}^T , \tag{20}$$

$$\bar{\mathbf{v}}_c' = \left\{ -\frac{1}{2} v_1 C_1^{-1}, \ldots, -\frac{1}{2} v_n C_n^{-1} \right\}^T , \tag{21}$$

$$\overline{\boldsymbol{\mathcal{A}}}_c = \{ \overline{\boldsymbol{\mathcal{A}}}_{\alpha\beta}^c \} , \quad \alpha, \beta = 1, \ldots, n$$

$$\overline{\boldsymbol{\mathcal{A}}}_{\alpha\beta}^c = \frac{1}{4} v_\alpha C_\alpha^{-1} \delta_{\alpha\beta} + \frac{1}{2} \sum_{\gamma=1}^{n} \left(A_\gamma^{\alpha\beta} - v_\alpha C_V^{-1} \sum_{\delta=1}^{n} C_\delta A_\gamma^{\delta\beta} \right) C_\gamma^{-1} . \tag{22}$$

The bounds (16) contain the conductivities C_α, volume fraction v_α of the phases, $A_\alpha^{\beta\gamma}$ describing the micro structure of the composite and the parameters $A_\alpha^{\beta\gamma}$ of this n-phase model in general d dimensions have been determined [8,9]

$$A_\alpha^{\beta\gamma} = \frac{d-1}{d} v_\alpha v_\beta v_\gamma \left(\sum_{\delta < \alpha} v_\delta \cdot \sum_{\kappa \le \alpha} v_\kappa \right)^{-1}, \beta, \gamma < \alpha,$$

$$A_\alpha^{\alpha\beta} = -\frac{d-1}{d} v_\alpha v_\beta \left(\sum_{\delta \le \alpha} v_\delta \right)^{-1}, \beta < \alpha, \tag{23}$$

$$A_\alpha^{\alpha\alpha} = \frac{d-1}{d} v_\alpha \sum_{\delta < \alpha} v_\delta \left(\sum_{\kappa \le \alpha} v_\kappa \right)^{-1}, \alpha \ge 2,$$

$$A_\alpha^{\beta\gamma} = 0 \quad \text{if} \quad \beta > \alpha \quad \text{or} \quad \gamma > \alpha \quad \text{or} \quad \alpha = \beta = \gamma = 1.$$

The three-point correlation parameters $A_\alpha^{\beta\gamma}$ of the model are determined as following

$$A_2^{11} = A_2^{22} = -A_2^{12} = -A_2^{21} = \frac{d-1}{d} \frac{v_1 v_2}{(v_1 + v_2)},$$

$$A_3^{11} = \frac{d-1}{d} \frac{v_1^2 v_3}{(v_1 + v_2)}, \quad A_3^{12} = A_3^{21} = \frac{d-1}{d} \frac{v_1 v_2 v_3}{(v_1 + v_2)},$$

$$A_3^{13} = A_3^{31} = -\frac{d-1}{d} v_1 v_3, \quad A_3^{22} = \frac{d-1}{d} \frac{v_2^2 v_3}{(v_1 + v_2)}, \tag{24}$$

$$A_3^{23} = A_3^{32} = -\frac{d-1}{d} v_2 v_3, \quad A_3^{33} = \frac{d-1}{d} v_3 (v_1 + v_2),$$

and other $A_\alpha^{\beta\gamma} = 0$. d is the dimension of the Euclidean space ($d = 2, 3$). In this particular case, the exact value of the effective transverse conductivity is determined when the upper and lower bounds coincide [4].

4. APPLICATIONS AND COMPARISONS

For numerical illustrations, consider some periodic models: square model (Fig. 3), hexagonal model (Fig. 4) and random model (Fig. 5). In random model, 60 coated-inclusion were planted randomly in a unit cell such that there is no circle overlapping. Coordinates of the center does not change but the outer radii change from 0.02 to 0.05 (corresponding volume fraction from 0.0754 to 0.4712).

Assume that the volume proportion between the phase I_1 and phase I_2 is constant ($v_{I_1}/v_{I_2} = 1$) for all three cases. We take $C_1 = 1$, $C_2 = 5$ and $C_3 = 20$. With them we can make 6 different combinations for the phases' conductivity. Figs. 6, 7 and 8 present the result for cases: $C_M = 1$, $C_{I_2} = 20$, $C_{I_1} = 5$; $C_M = 5$, $C_{I_2} = 1$, $C_{I_1} = 20$; $C_M = 20$, $C_{I_2} = 1$, $C_{I_1} = 5$ respectively. Exact value of doubly-coated circle model ($v_{I_1} = v_{I_2} = 0.1 \longrightarrow 0.45; v_M = 1 - 2v_{I_1}$) is also given for comparisons. Numerical simulations indicate that for doubly-coated (and multi-coated) circle assemblage model, the bounds
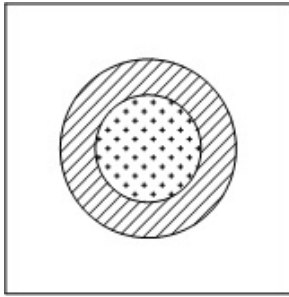
Fig. 3. Square model
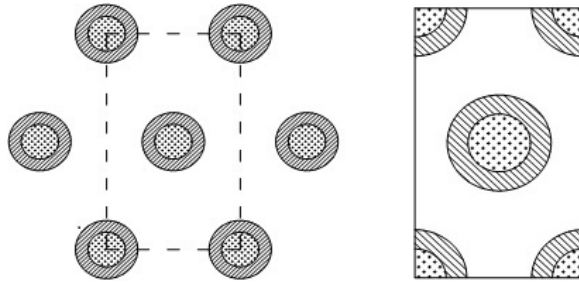
Fig. 4. Hexagonal model
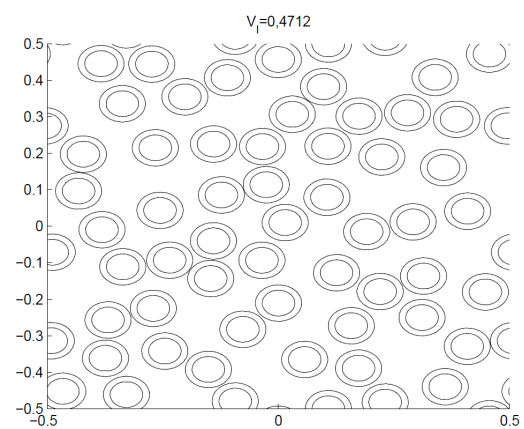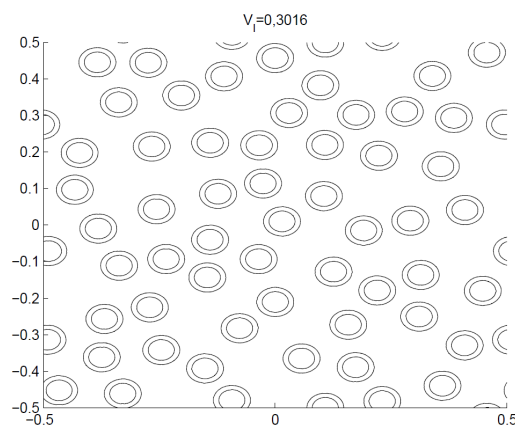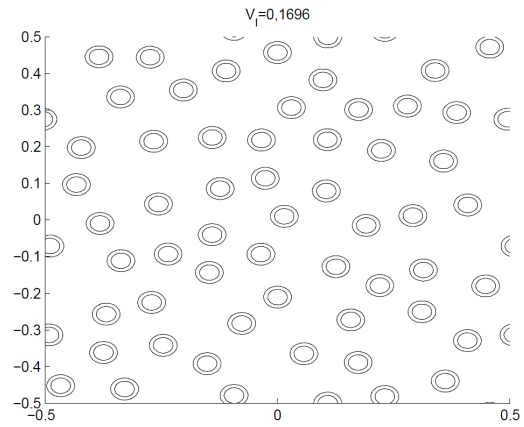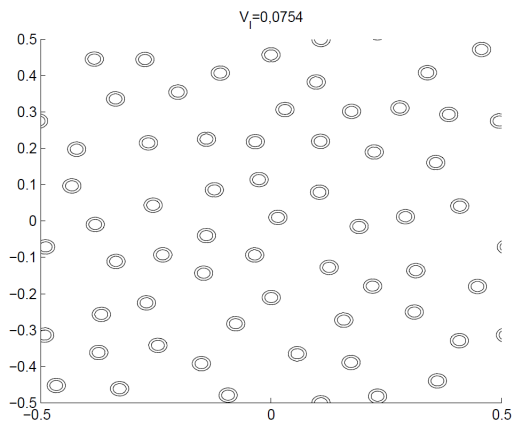
Fig. 5. Random model
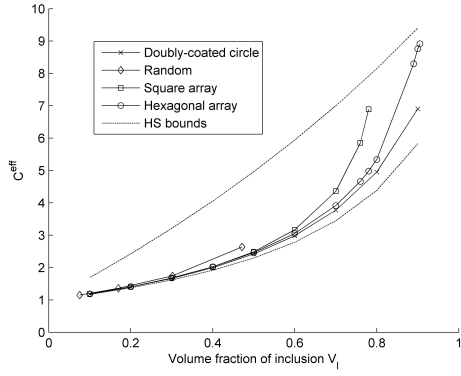
Fig. 6. Macroscopic conductivity for case $C_M = 1, C_{I_2} = 20, C_{I_1} = 5$
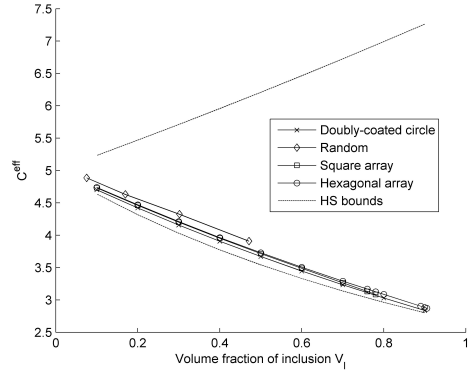
Fig. 7. Macroscopic conductivity for case $C_M = 5, C_{I_2} = 1, C_{I_1} = 20$
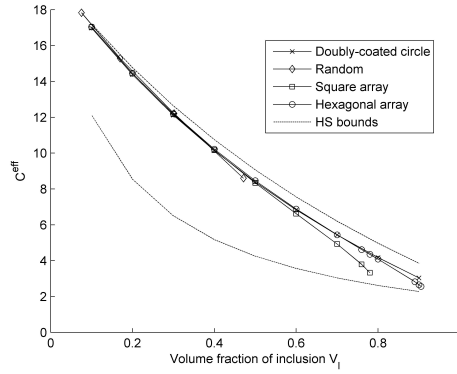
Fig. 8. Macroscopic conductivity for case $C_M = 20, C_{I_2} = 1, C_{I_1} = 5$

(16) converge to the exact effective conductivity, and we have an analytical expression of the conductivity for the model.

From Figs. 6, 7 and 8 one can see that: all the results fall inside the Hashin-Shtrikman' bounds as expected. When the volume fraction of the compounded inclusions is small-to-moderate (less than 30%), the model agrees well with the numerical results. When the volume fraction of the compounded inclusions increases, the numerical results diver from each other as well as from the model due to the influence of spatial distribution. The fact indicates the effect of the compound-inclusion interactions in close distances, which can not be accounted for by the idealistic coated circle model. The largest differences (compared to the model) appear in random model, followed by square and hexagonal models. At small volume fractions of compound spheres, the results appear to close to lower or upper HS bounds when the compound spheres appear more or less conductive than the matrix as discussed in [10]. However at large volume proportions of the coated

spheres the inclusions get close into each other, the influence of the matrix separating them becomes less dominant, and the results diver from the bounds as observed.

5. CONCLUSION

Macroscopic conductivity of three phases composites is determined using Fast-Fourier methods. Some periodic models are studied: square array, hexagonal array and random array. The numerical results of all models fall inside the Hashin-Shtrikman bounds. We observe that the simple multi-coated circle assemblage appears good when the volume proportion of the inclusions are from small to intermediate. At large volume fraction of inclusions, numerical simulations are needed for particular geometries to give more accurate evaluations of the effective conductivity, through practical microgeometry is generally hard to be described and incorporated into numerical scheme.

ACKNOWLEDGEMENTS

REFERENCES

[1] K. C. Le and D. C. Pham. Variational estimates of the effective thermal conductivities of transversely isotropic composites. *Journal of Engineering Physics*, **59**, (4), (1990), pp. 1245–1250.

[2] D. C. Pham. *Bounds on the macroscopic mechanical and physical properties of iso tropic multiphase materials*. PhD thesis, (1993).

[3] T.-K. Nguyen, V. Monchiet, and G. Bonnet. A Fourier based numerical method for computing the dynamic permeability of periodic porous media. *European Journal of Mechanics-B/Fluids*, **37**, (2013), pp. 90–98.

[4] N. T. Kien, N. V. Luat, and P. D. Chinh. Estimating effective conductivity of unidirectional transversely isotropic composites. *Vietnam Journal of Mechanics*, **35**, (3), (2013), pp. 203–213.

[5] G. Bonnet. Effective properties of elastic periodic composite media with fibers. *Journal of the Mechanics and Physics of Solids*, **55**, (5), (2007), pp. 881–899.

[6] J. C. Michel, H. Moulinec, and P. Suquet. Effective properties of composite materials with periodic microstructure: a computational approach. *Computer Methods in Applied Mechanics and Engineering*, **172**, (1), (1999), pp. 109–143.

[7] D. C. Pham. Bounds on the effective conductivity of statistically isotropic multicomponent materials and random cell polycrystals. *Journal of the Mechanics and Physics of Solids*, **59**, (3), (2011), pp. 497–510.

[8] D. C. Pham. Estimations for the overall properties of some locally-ordered composites. *Acta Mechanica*, **121**, (1-4), (1997), pp. 177–190.

[9] D. C. Pham and S. Torquato. Strong-contrast expansions and approximations for the effective conductivity of isotropic multiphase composites. *Journal of Applied Physics*, **94**, (10), (2003), pp. 6591–6602.

[10] M. Bornert, C. Stolz, and A. Zaoui. Morphologically representative pattern-based bounding in elasticity. *Journal of the Mechanics and Physics of Solids*, **44**, (3), (1996), pp. 307–331.